

## Biomorphic carbon materials coated meso-porous crystals

Jung Gyu Park<sup>a</sup>, Bijay Basnet<sup>a</sup>, Se Young Kim<sup>b</sup>, In Sub Han<sup>b</sup> and Ik Jin Kim<sup>a,\*</sup>

<sup>a</sup>Institute for Processing and Application of Inorganic Materials, (PAIM), Department of Materials Science and Engineering, Hanseo University, #46, Hanseo 1-ro, Haemi-myun, Seosan-si, Chungnam 31962, Korea

<sup>b</sup>Korea Institute of Energy Research (KIER), #152, Gajeong-gu, Daejeon 34129, Korea

A novel approach towards the formation of mesoporous template coated biomorphic carbon materials (BCM) was attempted by the application of two processing technique. BCM with honeycomb structure having the pore size of 15-25  $\mu\text{m}$  was developed by the carbonization method of natural wood, cypress. The three different templates were simultaneously synthesized and coated within BCM by an *in situ* hydrothermal process. All templates showed the single-phase nanocrystal which having the pore size of 3.45 nm for Linde type A zeolite, 11.09 nm for silicalite-1, and 10.95 nm for mesoporous silica, respectively. Their specific surface areas up to 65.97, 99.63, and 1.49  $\text{m}^2/\text{g}$ , respectively.

**Key words:** Biomorphic carbon, LTA zeolite, Silicalite-1, Mesoporous silica, Hydrothermal method.

### Introduction

Bioinspired natural wood has attained special interest due to their peculiar anatomical features, including hierarchical cellular morphology and oriented pore structure [1, 2]. During the last decades, several studies have focused on the synthesis of this class of materials by different routes [3]. The conversion of naturally available wood into biomorphic carbon material (BCM) with hierarchical and microcellular morphology is based on two processing approaches: substitution and transformation. Substitution is achieved by coating the inner surface of the plant tissue with oxidic precursors [4, 5]. BCM with unique structures can be obtained through pyrolysis of wood varieties such as *Chamaecyparis obtusa* (a.k.a. Cypress, Japanese cypress, Hinoki), *Pinus resinosa* (a.k.a. red pine), and *Picea* (a.k.a. spruce) [6], resulting in the production of a carbonaceous form. This form is then infiltrated and reacted with coated oxides and nanoxides to form a strong ceramic and a template composite that can be used for a variety of applications, including filtration and catalytic support for various potential technological applications. [7, 8]

Upon carbonization of wood such as cypress, red pine, and spruce, BCM containing many pores is produced. It can act as an effective base for the growth of carbon nanotubes (CNTs) at high temperatures [9-11]. It can also work as an adsorbent. To improve the surface area of BCM as filtration membrane and

catalyst substrate, the surface of the BCM should be modified to satisfy conditions for specific applications. For the surface modification of mesoporous template was selected such as Linde Type A (LTA) zeolite [12], silicalite-1 [13], and mesoporous silica [14]. Among these matrices, zeolites are excellent templates for supporting or encapsulating catalyst nanoparticles due to their well-defined pore structures and high surface areas [15], thereby leading to catalyst-particle stabilization and fine dispersion of nanoparticles.

Zeolites as templates are aluminosilicates with well-defined micropores that are responsible for unique properties of these materials, e.g., an ion exchange, separation, catalysis, and many new areas. However, in some cases, the sole presence of micropores limits the applicability of zeolites [3, 16]. Most importantly, different methods and materials are categorized to clearly illustrate recent progress in this field. Silicalite-1 has similar properties as zeolites [17]. Mesoporous structures are characterized by having a large specific surface area and pores with diameters between 2 and 50 nm. Among inorganic structures, mesoporous silica ( $\text{SiO}_2$ ) materials have been intensely studied as potential applications in catalysis, biological, biomedicine, and so on due to their outstanding characteristics, including availability for mass production and simple synthesis method [5, 13]. Mesoporous silica nanoparticles (MSNs) can be used as host materials for transporting therapeutic medications or encapsulating molecules [18]. They can be used as templates for the synthesis of CNTs. Good biocompatibility, high loading capacity, the possibility of attachment target ligands for specific cellular recognition or the design of well-defined and tunable porosity make MSNs suitable for drug delivery and carbon nanotube synthesis [6, 19].

\*Corresponding author:  
Tel : +82-41-660-1441  
Fax: +82-41-660-1441  
E-mail: [ijkim@hanseo.ac.kr](mailto:ijkim@hanseo.ac.kr)

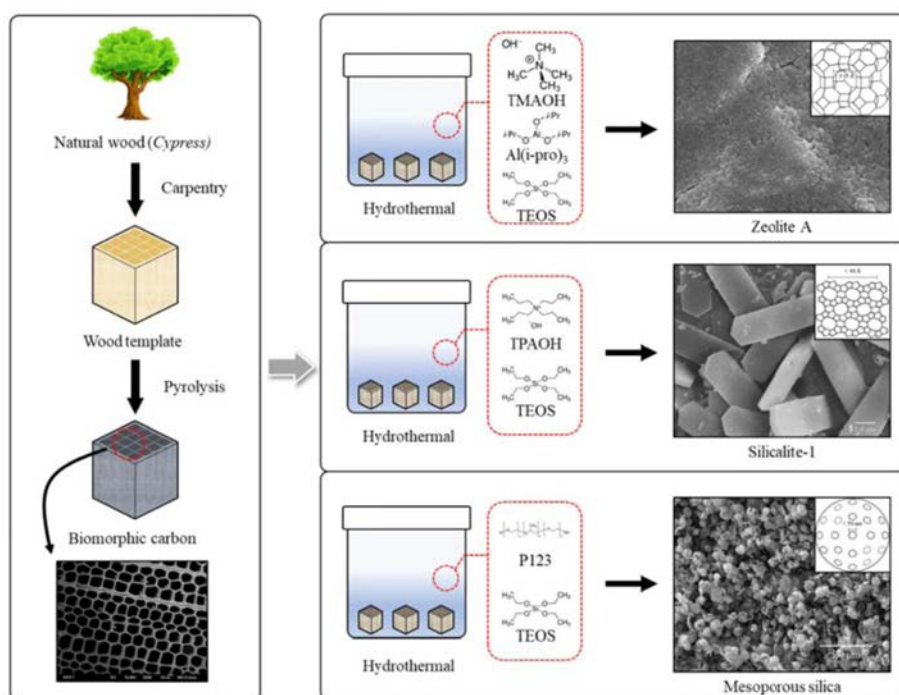


**Fig. 1.** Schematic diagram of the novel processing of coating, LTA Zeolite, silicalite-1 and mesoporous silica on BCM followed by carbonization process.

In this study, microporous BCM from natural wood, cypress was coated with LTA zeolite, silicalite-1, and mesoporous silica by hydrothermal method, respectively. For the characterization of BCM, field emission scanning electron microscope (FESEM), X-ray diffraction (XRD), thermogravimetric analysis (TGA) and Brunauer-Emmett-Teller (BET) were used.

## Experimental

### Raw materials

Natural wood cypress was carbonized to form a honeycomb porous carbon template. Aluminum isopropoxide ( $\text{Al}(\text{i-pro})_3$ , 98+ %), tetraethyl orthosilicate (TEOS, 98%), tetramethylammonium hydroxide (TMAOH, 25-% hydroxide solution), sodium hydroxide (NaOH) pellets (99.998%), and tetrapropylammonium hydroxide solution (TPAOH, 1.0M in  $\text{H}_2\text{O}$ ) were purchased from Sigma-Aldrich (St. Louis, MO, USA). They were used to synthesize LTA zeolite and silicalite-1 crystal. To synthesize mesoporous silica, poly(ethylene glycol)-block-poly(propylene glycol)-block-poly(ethylene glycol) (P123, Sigma-Aldrich), TEOS, and NaOH were used. Nitrogen gas ( $\text{N}_2$ , 99.99%) was purchased from Doekyang Co. Ltd. (South Korea). Deionized water and ethanol ( $\text{EtOH}$ , 94.5%) were obtained from Samchun Pure Chemical (South Korea).

### Preparation of BCM

BCM was prepared using the following steps. First, cypress samples with a square cross-section and

dimensions of  $10 \times 10 \times 20 \text{ mm}^3$  were prepared. These samples were then dried in an oven chamber at  $120^\circ\text{C}$  for 24 hrs. To maintain neutrality, carbon template was prepared by pyrolysis of Cypress specimens in the presence of inert gas. To avoid collapse of the sample during carbonizing process, samples were gently heated up to  $600^\circ\text{C}$  with a heating rate of  $0.5^\circ\text{C}/\text{min}$  for 6–8 hrs in a horizontal electric furnace with an  $\text{N}_2$  flow (10 sccm). Finally, the temperature was raised up to  $1000^\circ\text{C}$  at a heating rate of  $3^\circ\text{C}/\text{min}$  under a vacuum atmosphere followed by air-cooling to room temperature to accrue the porous carbon template as shown in Fig. 1(a).

### Mesoporous crystal synthesis and coating

To synthesize LTA zeolite, a mother solution of  $\text{Al}(\text{i-pro})_3$  : TEOS : TMAOH : NaOH :  $\text{H}_2\text{O}$  at molar ratio of 1 : 2.2 : 2.4 : 0.3 : 200 was prepared and then stirred for 8–12 hrs. The carbon template was then dipped into the zeolite mother solution and allowed to age for 12 hr. Afterward, this carbon template still in the zeolite mother solution was moved into a Teflon-lined stainless-steel pressure vessel wherein it was hydrothermally treated at  $90^\circ\text{C}$  for 3 days. Similarly, synthesis of silicalite-1 was obtained by a hydrothermal reaction using a mother solution of TPAOH : TEOS :  $\text{H}_2\text{O}$  at molar ratio of 1.5 : 7 : 360. TPAOH and  $\text{H}_2\text{O}$  were mixed stirred for 1.5 hrs. Then TEOS was added dropwise and stirred for 2 hrs. After that, the solution was moved to Teflon-lined stainless-steel pressure vessel. The carbon template was then dipped into a mother solution and allowed to age

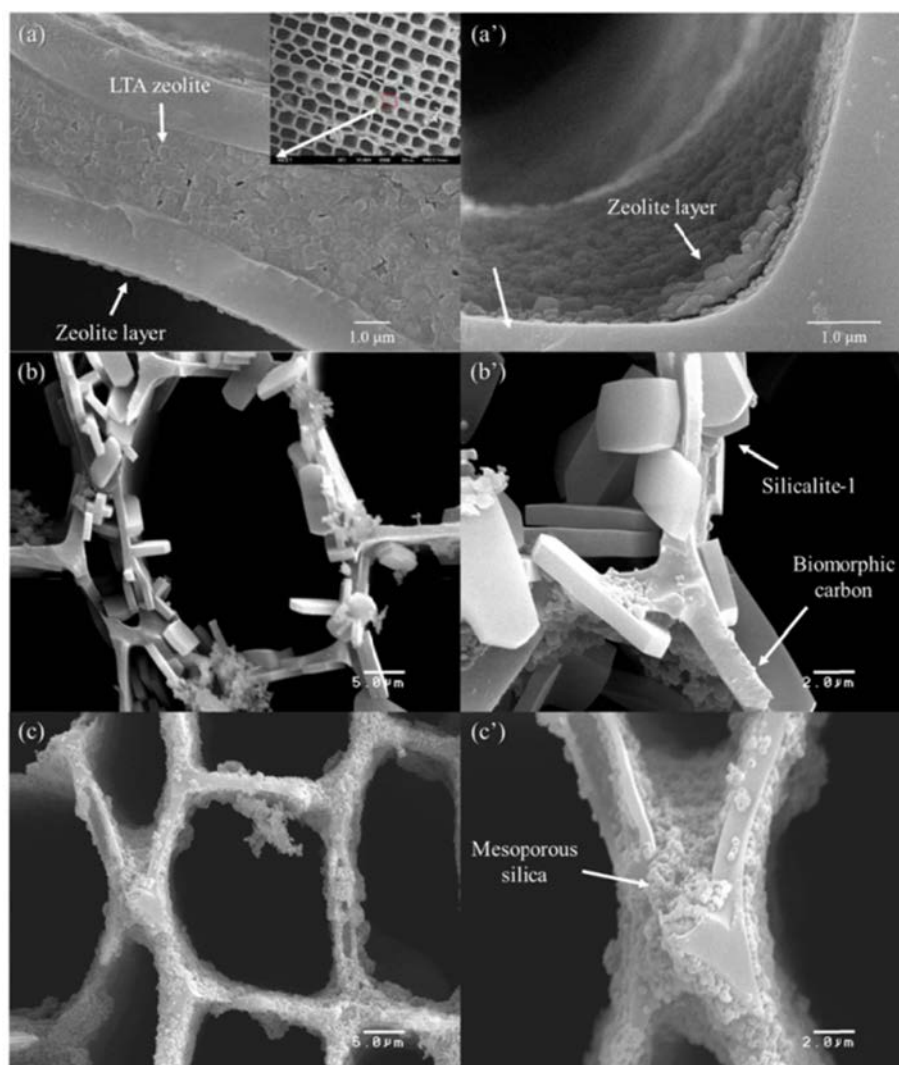


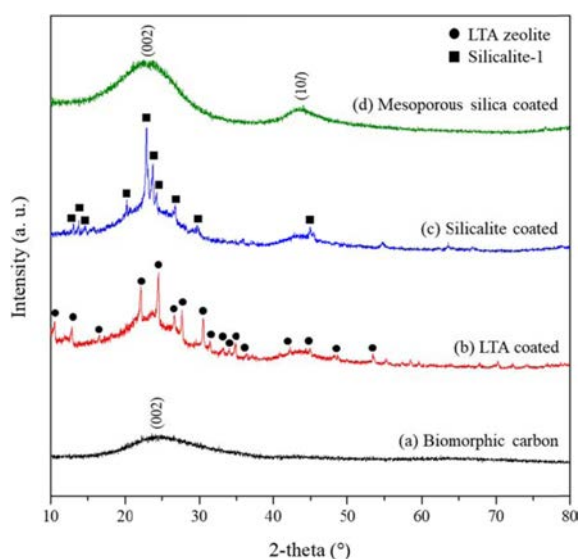
**Fig. 2.** FE-SEM images of cypress BCM coated with LTA (a), silicalite-1 (b), and mesoporous SiO<sub>2</sub> (c).

for 12 hrs. Finally, it was hydrothermally treated at 150 °C for 12 hrs. Mesoporous silica was synthesized from P123 : TEOS : NaOH : H<sub>2</sub>O at a molar ratio of 0.017 : 1 : 0.315 : 20. First, P123 was dissolved in H<sub>2</sub>O at 40 °C for 8 hrs. After P123 was fully dissolved, NaOH was added to the solution followed by stirring for 1.5 hrs. While maintaining agitation, TEOS was added dropwise at 40 °C for 12 hrs. After that, mother solution was moved to Teflon-lined stainless-steel pressure vessel and carbon template was dipped into the prepared solution for 12 hrs. Finally, the vessel was put in an oven at 120 °C for 8 hrs. Schematic diagram of the novel processing of coating, LTA Zeolite, silicalite-1, and mesoporous silica on BCM followed by carbonization process is shown in Fig. 1.

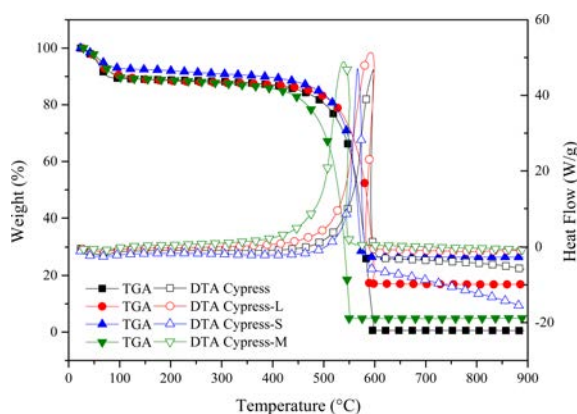
## Results and Discussion

Fig. 2 shows microstructures of (a) LTA type zeolite, (b) silicalite-1, and (c) mesoporous silica template coated cypress BCM. LTA zeolite was coated on

substrate with size of 150 nm to 300 nm in a configuration with a fine layer of well-controlled cube crystals. Fig. 2(a) and 2 (a') shows the cross-section FESEM images of BCM coated with LTA zeolite crystals. In general, LTA zeolite is generated by placing the cubic D4R units in the center of the edges of a cube. These well-shaped zeolite crystals are excellent template materials having the ordered framework structure with regular supercages ( $\alpha$ -cage) and channels of sub-nano size (4Å) for the encapsulation of (1-10 nm) particles [20, 21]. Fig. 2(b) and 2 (b') shows the FE-SEM images of BCM, coated with prismatic crystals morphology which is the characteristic feature of silicalite-1 single phase confirmed by XRD patterns (Fig. 3). As observed with higher magnification, the 5.0 μm silicalite-1 particles were entirely interlocked and coated on the surface of BCM. Fig. 2(c) and 2(c') show FE-SEM images of mesoporous silica film on the surface of BCM. The images revealed the presence of continuous and smooth mesoporous silica film layer of less than 1.0 μm.



**Fig. 3.** XRD patterns of BCM (a) and cypruss BCM coated with LTA (b), silicalite-1 (c), and mesoporous silica (d) template.



**Fig. 4.** TGA and DTA curves of template coated cypruss BCM.

Fig. 3 shows XRD plots of LTA, Silicalite-1, and mesoporous silica template synthesized on the surface of the BCM. As shown in these XRD plots, different peaks appeared, indicating monolayer and multi-layer fine coating of the template. These peaks were then compared to JCPDS files. Compared to JCPDS file # 97-002-4901, corresponding peaks reflected the yield of LTA phase,  $2\theta = 10^\circ$  (220), and  $24^\circ$  (600). A single phase with an average lattice constant of  $24.61 \text{ \AA}$  was found in the obtained XRD. This is a simple cubic arrangement of eight tetrahedral with D4R [21]. Similarly, when obtained XRD plots were compared to

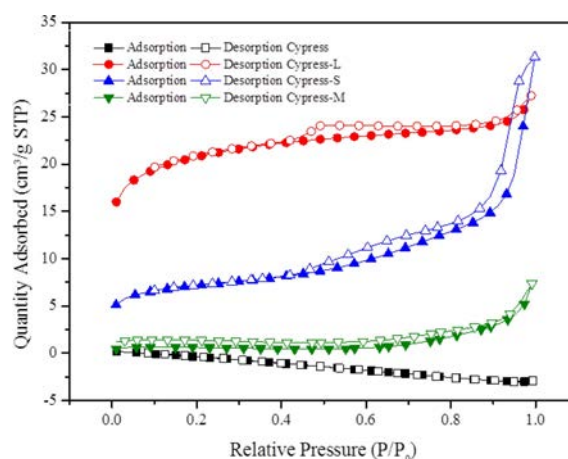


**Fig. 5.** BET analysis of template coated cypruss BCM.

JCPDS 42-0023 original JCPDS file for silicalite-1, corresponding peaks were also found. This assures the synthesis of silicalite-1 in the BCM. Randomly oriented silicalite-1 crystals were coated as shown in Fig. 2(b). BCM was also coated with mesoporous silica. However, it was hard to recognize it with wide-angle XRD due to mesoporous silica's properties. It must be analyzed with small angle XRD [22]. The peak intensity was the background of amorphous carbon.

Fig. 4. shows DTA-TGA curves of BCM coated with LTA, silicalite-1, and mesoporous silica template. BCM was burned from  $400^\circ\text{C}$  to  $600^\circ\text{C}$  to check the temperature with continuous heat flow. Since templates (LTA, silicalite-1, mesoporous silica) were not burned in the  $\text{N}_2$  atmosphere, remain weight was compared with filled black one to obtain coating yield. DTA only represents BCM burned out in  $\text{N}_2$  atmosphere with exothermic reaction while the synthesized template remained unchanged. Maximum yields of silicalite-1, LTA, and mesoporous silica were found to be 25.98%, 16.45%, and 4.25%, respectively.

Fig. 5 shows  $\text{N}_2$ -adsorption/desorption isotherms of BCM coated with LTA, silicalite-1, or mesoporous silica. According to the International Union of Pure and Applied Chemistry (IUPAC) classification, isotherms of all samples studied belonged to type IV [23], suggesting that these adsorbents are mesoporous materials. Capillary condensation phenomenon may occur in their pore channels. As illustrated in Fig. 5, the  $\text{N}_2$  adsorption capacity of silicalite-1 seems to be

**Table 1.** BET surface and yield of template coated cypruss BCM.

Sample	The pore size of template [nm]	Mean crystal size [ $\mu\text{m}$ ]	BET surface area [ $\text{m}^2/\text{g}$ ]	The yield of templates [%]
Cypress	—	—	2.1266	—
Cypress-L	3.456	0.247	65.9778	16.3503
Cypress-S	11.095	7.524	99.6346	25.9403
Cypress-M	10.953	0.381	1.4965	4.3943

greater than that of LTA zeolite or mesoporous silica. This is probably because pores of LTA zeolite and mesoporous silica are partially covered by the active ingredient [24], thus reducing the surface area. Furthermore, the hysteresis loop shifts in the relative pressure range of 0.4-1.0. BET isotherms graphs (Fig. 5.) showed a typical type (IV) with type II like hysteresis loops, indicating the presence of mesopores in all samples (LTA zeolite, silicalite-1, mesoporous silica). The position of inflection point of  $P/P_0$  is related to the diameter of mesoporous range. The sharpness of the step shows uniform mesoporous size distribution. Results of BET and yield are summarized in Table 1. Templates were coated on BCM to increase specific surface area, especially silicalite-1. BET surface areas of original carbonized cypress, LTA zeolite, silicalite-1, and mesoporous silica were 2.126, 65.977, 99.634, and 1.496 m<sup>2</sup>/g, respectively (Table 1).

### Conclusions

Microporous BCM with the pore size of 15-25 μm was achieved by carbonization method. LTA zeolite, silicalite-1, and mesoporous silica were synthesized by hydrothermal method and finely coated as single-phase nanocrystals on BCM. These single-phase and nano sized LTA, silicalite-1 were coated with respective peaks as identified by XRD analysis. Mesoporous silica was found to be amorphous. Silicalite-1 was found to have the highest yield at 25.98%, followed by LTA at 16.45% and mesoporous silica at 4.39%. LTA zeolite was synthesized with surface area up to 99.65 m<sup>2</sup>/g while mesoporous silica was found to have the lowest surface improvement with surface area of only 1.50 m<sup>2</sup>/g. The pore size of LTA (3.456 nm), silicalite-1 (11.095 nm), and mesoporous silica (10.953 nm) as template is an important factor in carbon nanotube synthesis and growth. It could control catalysis nanoparticle sizes and loaded homogeneously distribution onto BCM substrates.

### Acknowledgments

This research was supported by Basic Science Research Program through the National Research

Foundation of Korea (NRF) funded by the Ministry of Education (NRF-2018R1D1A1B07049071).

### References

1. Y. Hu, C. Liu, Y. Zhang, N. Ren, Y. Tang, *Microporous Mesoporous Mater.* 119 (2009) 306-314.
2. R. Zhao, J. Chen, J. Liu, J. Fan, J. Du, *Mater. Lett.* 139 (2014) 494-497.
3. K. Zhuang, G. Yin, X. Pu, X. Chen, X. Liao, Z. Huang, Y. Yao, *MRS Commun.* 6 (2016) 449-454.
4. I.G. Werten, P.T. Dharmawijaya, P.T.P. Aryanti, R.R. Mukti, Khoiruddin, *RCS Adv.* 7 (2017) 29520-29539.
5. N. Tijani, H. Ahlafi, M. Smahih, A.E. Mansouri, *Mediterr. J. Chem.* 2 (2013) 484-492.
6. A.I. Lupulescu, J.D. Rimer, *Science* 344, (2014) 729-731.
7. R. Dragomirova, S. Wohlrab, *Catalysts* 5 (2015) 2161-2222.
8. S.I. Zones, H. Lee, M.E. Davis, J. Casci, A.W. Burton, *Stud. Surf. Sci. Catal.* 158 (2005) 1-10.
9. A. Sundblom, A.E.C. Palmqvist, K. Holmberg, *Langmuir* 26 (2010) 1983-1990.
10. S.Y. Chen, S. Cheng, *Chem. Mater.* 19 (2007) 3041-3051.
11. Q. Wei, Z.R. Nie, Y.L. Hao, L. Liu, Z.X. Chen, J.X. Zou, *J. Sol-Gel Sci. Technol.* 39 (2006) 103-109.
12. H. Mori, K. Aotani, N. Sano, H. Tamon, *J. Mater. Chem.* 21 (2011) 5677-5681.
13. J.P. Hanarahan, A. Donovan, M.A. Morris, J.D. Holmes, *J. Mater. Chem.* 17 (2007) 3881-3887.
14. P. Gao, M. Wu, B. Li, Y. Liu, *Mater. Res. Bull.* 44 (2009) 644-648.
15. P. Gao, Y. Bai, S. Lin, W. Guo, H. Xiao, *Ceram. Intl.* 34 (2008) 1975-1981.
16. M. Adam, M. Oschatz, W. Nickel, S. Kaskel, *Microporous Mesoporous Mater.* 210 (2015) 26-31.
17. A. Chourdary, S.K. Pratihar, S.K. Behera, *RSC Adv.* 6 (2016) 95897-95902.
18. R.J. Sun, W.Q. Wang, Y.Q. Wen and X. Zhang, *Nanomaterials* 5 (2015) 2019-2053.
19. M. Vallet-Regí, M. Colilla, I. Izquierdo-Barba and M. Manzano, *Molecules* (2018) 1-19.
20. J. Kim, W. Zhao, J.H. Chung, M. Olarinc, A.F. Trandabat and R.C. Ciobanac, *Journal of Ceramic Processing Research* 11[3] (2010) 303-307.
21. Y.M. Kim, J.H. Chang and I.J. Kim, *Journal of Ceramic Processing Research* 10[4] (2009) 453-456.
22. W. Harrison, G. Erastus, K. Paul, Z. Tang and Y. Gao, *African Journal of Pharmacy and Pharmacology* 5[21] (2011) 2402-2410.
23. K. Sing, *Colloids and Surfaces A: Physicochemical and Engineering Aspects* 187-188 (2001) 3-9.
24. S.V. Boycheva and D.M. Zgureva, *Bulgarian Chemical Communications, Special Issue A* (2016) 101-107